PHYSICAL REVIEW D **91,** 014022 (2015)

Search for top quark flavor changing neutral currents in same-sign top quark production

Reza Goldouzian*

School of Particles and Accelerators, Institute for Research in Fundamental Sciences (IPM), P.O. Box 19395-5531, Tehran, Iran

(Received 23 November 2014; published 21 January 2015)

The presence of the anomalous top-quark flavor-changing neutral-current (FCNC) interactions leads to the production of same-sign top quarks in proton-proton collisions. The results of a search for events with same-sign dileptons and b jets conducted by the CMS Collaboration with 10.5 fb^{-1} of data collected in pp collisions at $\sqrt{s} = 8$ TeV are used to obtain the constraints on the strength of top-quark FCNC interactions. The 95% confidence level upper limits on the branching ratios of top-quark decays to a light quark $q = u, c$ and a gauge or a Higgs boson are set to be $\text{BR}(t \to u\gamma) < 1.27\%$, $\text{BR}(t \to uZ) < 0.8\%$, $\text{BR}(t \to ug) < 1.02\%$, and $\text{BR}(t \to uH) < 4.21\%$. The sensitivity of future searches in the same-sign top-quark channel is also presented.

DOI: 10.1103/PhysRevD.91.014022 PACS numbers: 14.65.Ha, 12.39.Hg

I. INTRODUCTION

Because of the large mass of the top quark near the electroweak symmetry-breaking scale, the study of top-quark properties can open a unique window to new physics [1]. In the Standard Model (SM) framework, the flavor-changing neutral-current (FCNC) processes are forbidden at tree level and are suppressed at the level of quantum loop corrections due to the Glashow-Iliopoulos-Maiani (GIM) mechanism [2]. Whereas the SM predicts tiny branching ratios of top-quark FCNC decays to a light up-type quark and a gauge or Higgs boson [3] [$\text{BR}(t \to qX) \sim 10^{-17}$–$10^{-12}$, where $q =$ up or charm quark and $X =$ photon (γ), Z boson (Z), gluon (g), or Higgs boson (H)], various extensions of the SM predict a huge enhancement for the branching ratios of these decays by relaxing the GIM suppression and introducing new particles that contribute in the quantum loops [4–9]. It indicates that the observation of any sign from top-quark FCNC processes will give evidence of physics beyond the SM.

Over the years, different experiments have searched for FCNC processes in the anomalous decays of top quarks in $t\bar{t}$ events or anomalous productions of single top events. They have observed no clear evidence of the presence of the FCNC processes and the exclusion limits are set on the branching ratios of anomalous top decays. In Table I the most stringent limits obtained in hadron colliders from different sensitive channels are shown. Although the SM predicts top-quark anomalous branching ratios many orders of magnitude below the current experimental limits, experiments are closing in on the regions that are available to physics beyond the SM.

In addition to the anomalous production or decays of top quarks, the FCNC interactions can result in the appearance of a same-sign top quark in hadron colliders [22–24]. Figure 1 displays the representative diagrams describing the anomalous same-sign top-quark production. Same-sign top production followed by the leptonic decay of a W boson from top decays gives rise to a final state with same-sign leptons and b jets. Despite the small cross section of the signal channels due to the presence of two anomalous vertices for tt production, this final state has been shown to have very little SM background and is sensitive to new-physics effects [25,26]. Therefore, a same-sign dilepton final state would provide a new window for searching for FCNC interactions.

To investigate the utility of same-sign top production in searching for FCNC interactions, we make use of the results of a search for new physics in events with same-sign dileptons and b jets performed with 10.5 fb^{-1} of data collected from 8 TeV pp collisions by the CMS Collaboration to estimate the upper limit on the strength of the top FCNC anomalous couplings [27].

In this work, we study various processes that contribute to the same-sign top-quark final state through tqX vertices, where $X = H$, γ, Z, or a gluon. We limit the strength of the FCNC anomalous couplings by considering the leptonic decay of a W boson from top-quark decay and using same-sign dilepton experimental results.

The organization of this paper is as follows. Section II describes the theoretical framework used to search for FCNC processes. In Sec. III we review the CMS same-sign dilepton search and the simulation details of signal samples. The results of the same-sign dilepton search are interpreted in terms of the strength of FCNC interactions in Sec. IV. The prediction of 95% C.L. exclusion limits at the 14 TeV LHC in Sec. V is followed by a conclusion in Sec. VI.

*r.goldouzian@ipm.ir

TABLE I. The most stringent experimental bounds on FCNC branching ratios obtained in Tevatron and LHC experiments.

	CDF	D0	ATLAS	CMS
BR$(t \to q\gamma)\%$	3.2 [10]	-	-	0.016 [11]
BR$(t \to qZ)\%$	3.7 [12]	3.2 [13]	0.73 [14]	0.05 [15]
BR$(t \to qg)\%$	0.039 [16]	0.02 [17]	0.0031 [18]	0.035 [19]
BR$(t \to qH)\%$	-	-	0.79 [20]	0.56 [21]

II. ANOMALOUS FLAVOR-CHANGING TOP-QUARK COUPLINGS

Top-quark anomalous interactions can be described in a model-independent way by an effective Lagrangian [3]. The most general effective Lagrangain describing the interactions between the top quark and a light up-type quark (u or c) and a gauge or Higgs boson emerging from dimension-six operators can be written as

$$\begin{aligned}-\mathcal{L}_{\text{eff}} &= e\kappa_{q\gamma}\bar{q}\frac{i\sigma^{\mu\nu}q_\nu}{\Lambda}[\gamma_L P_L + \gamma_R P_R]tA_\mu \\ &+ \frac{g}{2cos\theta_w}\kappa_{qZ}\bar{q}\frac{i\sigma^{\mu\nu}q_\nu}{\Lambda}[z_L P_L + z_R P_R]tZ_\mu \\ &+ g_s\kappa_{qg}\bar{q}\frac{i\sigma^{\mu\nu}q_\nu}{\Lambda}[g_L P_L + g_R P_R]T^a tG_{a\mu} \\ &+ \kappa_{qH}\bar{q}[h_L P_L + h_R P_R]tH + \text{H.c.}, \end{aligned} \quad (1)$$

where e is the electron charge, g is the weak-coupling constant, g_s is the strong-coupling constant, θ_w is the Weinberg angle, $P_{L,R} = \frac{1}{2}(1 \mp \gamma^5)$, $\sigma^{\mu\nu} = \frac{1}{2}[\gamma^\mu, \gamma^\nu]$, and the symbols $\bar{q}$ and t represent the up- (or charm-) and top-quark spinor fields. The parameters $\kappa_{q\gamma}$, κ_{qZ}, κ_{qg}, and κ_{qH} define the strength of the real and positive anomalous couplings for the current with a photon, Z boson, gluon, or Higgs boson, respectively. The relative contribution of the left and right currents are determined by $\gamma_{L,R}$, $z_{L,R}$, $g_{L,R}$, and $h_{L,R}$, which are normalized as $|\gamma_L|^2 + |\gamma_R|^2 = 1$, $|z_L|^2 + |z_R|^2 = 1$, etc. In the Lagrangian, q is the momentum of the gauge or Higgs boson and Λ is the new physics cutoff which by convention is set to the top-quark mass.

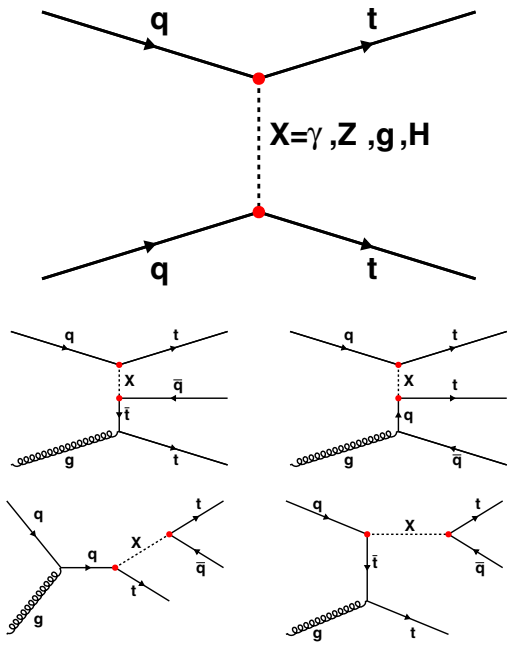

FIG. 1 (color online). Feynman diagrams describing the production of same-sign top-quark productions (top) and same-sign top + $\bar{q}$ production (bottom) representative of same-sign top + 1 jet diagrams due to FCNC interactions ($q = u$ or c).

In the literature, there are many alternatives for normalizing the coupling constants in $\mathcal{L}_{\text{eff}}$. Therefore, we will use the top-quark branching ratio to express our results to make it comparable with other experimental results. The tree-level prediction for the top-quark decay rate to the W boson and massless b quark is [3]

$$\Gamma(t \to Wb) = \frac{\alpha}{16 s_w^2}|V_{tb}|^2 \frac{m_t^3}{m_W^2}\left[1 - 3\frac{m_W^4}{m_t^4} + 2\frac{m_W^6}{m_t^6}\right]. \quad (2)$$

The partial decay widths of the top quark with flavor-violating interactions are given by

$$\begin{aligned}\Gamma(t \to q\gamma) &= \frac{\alpha}{4} m_t^3 \frac{|\kappa_{q\gamma}|^2}{\Lambda^2}, \\ \Gamma(t \to qZ) &= \frac{\alpha}{32 s_W^2 c_W^2} m_t^3 \frac{|\kappa_{qZ}|^2}{\Lambda^2}\left[1 - \frac{m_Z^2}{m_t^2}\right]^2\left[2 + \frac{m_Z^2}{m_t^2}\right], \\ \Gamma(t \to qg) &= \frac{\alpha_s}{3} m_t^3 \frac{|\kappa_{qg}|^2}{\Lambda^2}, \\ \Gamma(t \to qH) &= \frac{1}{32\pi} m_t |\kappa_{qH}|^2\left[1 - \frac{m_H^2}{m_t^2}\right]^2. \end{aligned} \quad (3)$$

For numerical calculations we set $m_t = 172.5$ GeV, $m_Z = 91.2$ GeV, $m_H = 125$ GeV, $s_W^2 = 0.234$, $\alpha_s = 0.108$, and $\alpha = 1/128.92$.

III. A SAME-SIGN TOP PRODUCTION SEARCH FOR TOP-QUARK FCNC INTERACTIONS

A. Experimental input

Same-sign dilepton searches at hadron colliders can provide great sensitivity for probing many new-physics models [28–31]. In this work we follow and use the results of the same-sign dilepton and b-jet search strategies adopted by the CMS Collaboration [27].

In the analysis two isolated same-sign leptons (e or μ) with $P_T > 20$ and $|\eta| < 2.4$ ($1.442 < |\eta| < 1.566$ is excluded for the electron) are required. More criteria on the events with a third lepton are applied to minimize the contribution of backgrounds with $\gamma^* \to l^+ l^-$ and low-mass bound-state and multiboson production. In the CMS report, the lepton identification efficiency, isolation cuts, and

TABLE II. A summary of the results. For each signal region (SR) the kinematic requirements, the prediction for the total background (BG), and the observed number of events are shown. The 95% C.L. upper limit on the number of new-physics events under the assumption of 30% uncertainty on the signal efficiency is shown in the last row. Note that the number of jets in the first line of the table includes both b-tagged and non-b-tagged jets.

	SR0	SR1	SR2	SR3	SR4	SR5	SR6	SR7	SR8
No. of jets (b jets)	$\geq 2(\geq 2)$	$\geq 2(\geq 2)$	$\geq 2(\geq 2)$	$\geq 4(\geq 2)$	$\geq 4(\geq 2)$	$\geq 4(\geq 2)$	$\geq 4(\geq 2)$	$\geq 3(\geq 3)$	$\geq 4(\geq 2)$
lepton charges	$++/--$	$++/--$	$++$	$++/--$	$++/--$	$++/--$	$++/--$	$++/--$	$++/--$
E_T^{miss}	≥ 0 GeV	≥ 30 GeV	≥ 30 GeV	≥ 120 GeV	≥ 50 GeV	≥ 50 GeV	≥ 120 GeV	≥ 50 GeV	≥ 0 GeV
H_T	≥ 80 GeV	≥ 80 GeV	≥ 80 GeV	≥ 200 GeV	≥ 200 GeV	≥ 320 GeV	≥ 320 GeV	≥ 200 GeV	≥ 320 GeV
No. of BG	40 ± 14	32 ± 11	17.7 ± 6.1	2.2 ± 1.0	8.1 ± 3.4	5.7 ± 2.4	1.7 ± 0.7	1.2 ± 0.6	8.1 ± 3.3
No. of data	43	38	14	1	10	7	1	1	9
No. of NP(30% unc.)	30.4	29.6	10.7	3.8	12	9.6	3.9	4	10.5

detector effects were combined. The lepton selection efficiency is parametrized as [27]

$$\epsilon = \epsilon_\infty \text{erf}\left(\frac{p_T - 20\ \text{GeV}}{\sigma}\right) + \epsilon_{20}\left[1 - \text{erf}\left(\frac{p_T - 20\ \text{GeV}}{\sigma}\right)\right], \quad (4)$$

with $\epsilon_\infty = 0.65(0.69)$, $\epsilon_{20} = 0.35(0.48)$, and $\sigma = 42$ GeV (25 GeV) for electrons (muons).

Jets are clustered using the anti-k_t algorithm [32]. At least two jets with $P_T > 40$ and $|\eta| < 2.4$ are needed. b tagging is defined using the combined secondary vertex which uses the information of the secondary vertex and the track-based lifetime [33]. The b-tag efficiency is evaluated to be 0.71 for the b jets with $90 < p_T < 170$ GeV, and at higher (lower) p_T it decreases linearly with a slope of -0.0004 (-0.0047) GeV^{-1} [27]. Candidate events are required to have at least two b-tagged jets. Finally, in different signal regions different cuts are applied on the scalar sum of the transverse momenta of jets (H_T) and the missing transverse energy (E_T^{miss}).

This search divides same-sign dilepton events into several categories, based on the charge of the leptons, the number of selected b jets, and number of selected jets, H_T and E_T^{miss}. Table II shows the kinematic requirements, the total background, the observed data, and the upper limit on the number of new-physics events of nine signal regions. The signal regions are not independent and have some overlap with one another, so one cannot combine the limits from different regions.

B. Signal channels and simulation details

The presence of FCNC interactions leads to the production of tt and $\bar{t}\bar{t}$ through tuX or tcX interactions in proton-proton collisions. The Lagrangian in Eq. (1) is implemented in FeynRules [34] and passed to the MadGraph5 [35] framework by means of the UFO model [36]. The implementation of the leading-order cross section calculated by MadGraph is validated for various couplings by comparing the tX production cross sections calculated by protos [37].

Due to the larger parton distribution function (PDF) of the u quark (valance quark) in the proton compared to the c, $\bar{c}$, and $\bar{u}$ quarks (sea quarks), the main contribution to the cross section comes from the tt production through an anomalous tuX interaction, and the contributions of other signal channels are small [38]. In Table III the cross sections of different signal channels are compared, while CTEQ6L1 is used to evaluate the parton densities.

In Fig. 2 we plot the cross section of the anomalous production of same-sign top quarks for the LHC at 8 TeV against the branching ratio of the top-quark FCNC decays. We show the tt cross section originating from different anomalous interactions separately. The red curve corresponds to the tug anomalous coupling, while other anomalous couplings are set to zero. As can be seen, any bound on the production of same-sign top quarks (which is available

TABLE III. Same-sign top production cross section due to an anomalous photon, Z-boson, gluon, or Higgs exchange at the LHC for $\sqrt{s} = 8$ TeV as a function of anomalous couplings. No cut is implemented on the final-state top quarks. CTEQ6L1 is used to evaluate the parton densities, while the renormalization scale μ_R and factorization scale μ_F are fixed at $\mu_R = \sqrt{\hat{s}} = \mu_F$. Note that the $pp \to tt + \text{jet}$ processes are not included.

	$pp \to tt$	$pp \to \bar{t}\bar{t}$
$tq\gamma$	$101.25\kappa_{u\gamma}^4 + 9.60\kappa_{u\gamma}^2\kappa_{c\gamma}^2 + 0.12\kappa_{c\gamma}^4$ (pb)	$0.8\kappa_{u\gamma}^4 + 0.65\kappa_{u\gamma}^2\kappa_{c\gamma}^2 + 0.12\kappa_{c\gamma}^4$ (pb)
tqZ	$179.85\kappa_{uZ}^4 + 15.17\kappa_{uZ}^2\kappa_{uZ}^2 + 0.22\kappa_{cZ}^4$ (pb)	$1.3\kappa_{uZ}^4 + 1.01\kappa_{uZ}^2\kappa_{uZ}^2 + 0.22\kappa_{cZ}^4$ (pb)
tqg	$44.35\kappa_{ug}^4 + 4.57\kappa_{ug}^2\kappa_{cg}^2 + 0.05\kappa_{cg}^4$ (nb)	$0.4\kappa_{ug}^4 + 0.32\kappa_{ug}^2\kappa_{cg}^2 + 0.05\kappa_{cg}^4$ (nb)
tqH	$14.02\kappa_{uH}^4 + 4.45\kappa_{uH}^2\kappa_{cH}^2 + 0.11\kappa_{cH}^4$ (pb)	$0.52\kappa_{uH}^4 + 0.47\kappa_{uH}^2\kappa_{cH}^2 + 0.11\kappa_{cH}^4$ (pb)

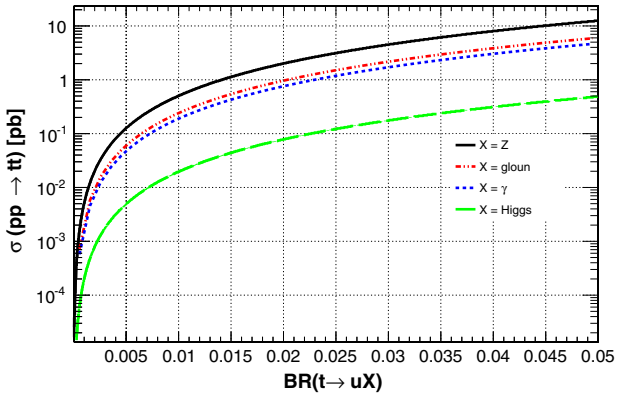

FIG. 2 (color online). Anomalous top pair production cross section for the process $pp \to tt$ due to tuX anomalous vertices versus the FCNC branching ratios for the decays $\mathrm{BR}(t \to u\gamma)$, $\mathrm{BR}(t \to uZ)$, $\mathrm{BR}(t \to ug)$ and $\mathrm{BR}(t \to uH)$.

from the LHC results) immediately implies a bound on the anomalous top FCNC decays. Another interesting observation from Fig. 2 is the relative sensitivity of the FCNC top-quark decays due to a photon, Z-boson, gluon, or Higgs exchange to same-sign top pair production.

Four separated samples of 100 000 events are generated independently corresponding to anomalous tt production through FCNC interactions. In the production of the signal events, the top-quark branching ratio to a bottom quark and a W boson is assumed to be 100%. Then the W boson is required to decay only into a charge lepton (e, μ, or τ) and a neutrino in MADGRAPH to ensure good statistical coverage and include leptonic tau decays. PYTHIA [39] is used to simulate the subsequent showering and hadronization effects. Detector effects are simulated using DELPHES [40]. The DELPHES card for simulating the CMS detector is modified in order to include the lepton and b-tag efficiencies calculated by the CMS Collaboration, as discussed in the previous section.

We analyze each signal channel separately. The CMS same-sign lepton search is closely followed to determine the efficiency for FCNC signal events passing the selections. Similar cuts are applied on the selected leptons, jets, b jets, H_T, and E_T^{miss} from simulated signal samples.

IV. RESULTS

The same-sign dilepton final state coming from $t \to Wb \to l\nu b$ in same-sign top production is associated with two b jets and missing transverse energy from the undetected neutrinos. In addition, the signal samples are dominated by the events with positive charged leptons, as discussed in the previous section. Therefore, the most sensitive signal region in our search for FCNC interactions is SR2. In this category, the signal efficiency is high, while the SM backgrounds and their uncertainties are small compared to other signal regions. In other words, the best significance is obtained from SR2.

As no excess above the SM expectation is observed, the 95% C.L. upper bound on the number of new-physics events were set in Ref. [25]. In Table II the bounds are shown in each of the nine signal regions. In order to determine more conservative upper bounds, the results considering a 30% uncertainty on the signal efficiency are chosen between 10, 20, and 30%.

The results for the signal region SR2 are used to set the limit on the FCNC anomalous couplings. In the derivation of the limits, the contributions of $tq\gamma$, tqZ, tqg, and tqH to same-sign top production are considered separately. Therefore, the limits are evaluated on one of the FCNC couplings, while setting the other couplings to zero. The limits on the strength of FCNC anomalous couplings can be converted to limits on the anomalous top-quark decays and are summarized in Table IV.

Figures 3 and 4 show the 95% C.L. excluded region in the $(\kappa_{uX}, \kappa_{cX})$ and $(\mathrm{BR}(t \to uX), \mathrm{BR}(t \to cX))$ plane obtained by this analysis. Due to the PDF of the proton, the LHC data are less sensitive to the κ_{cX} parameter than κ_{uX}.

V. SENSITIVITY AT THE 14 TeV LHC

In this section, we study the sensitivity of future searches for FCNC interactions through same-sign top-quark production. In Fig. 5, the cross sections for tt production induced by flavor-violating top-Z, top-photon, top-gluon, and top-Higgs couplings normalized to the corresponding top-quark decay branching ratios are shown as a function of the center-of-mass energy. We find from Fig. 5 that for a given value of $BR(t- > qX)$ FCNC branching ratios, the anomalous tZq coupling is the most sensitive coupling, followed by tqg, $tq\gamma$, and tqH in the shown range of the center-of-mass energy. The cross sections of all signal channels increase by increasing the center-of-mass energy and the cross section due to the fact that tqH increases less than the others.

TABLE IV. The observed 95% upper limits on the top-quark FCNC anomalous couplings and branching ratios.

Process (tqX)	$\kappa_{uX}(\kappa_{cX} = 0)$	$\kappa_{cX}(\kappa_{uX} = 0)$	$\mathrm{BR}(t \to uX)(\%)$	$\mathrm{BR}(t \to cX)(\%)$
$tq\gamma$	0.23	1.28	1.27	38.15
tqZ	0.20	1.15	0.80	25.52
tqg	0.05	0.25	1.02	27.73
tqH	0.39	1.30	4.21	45.46

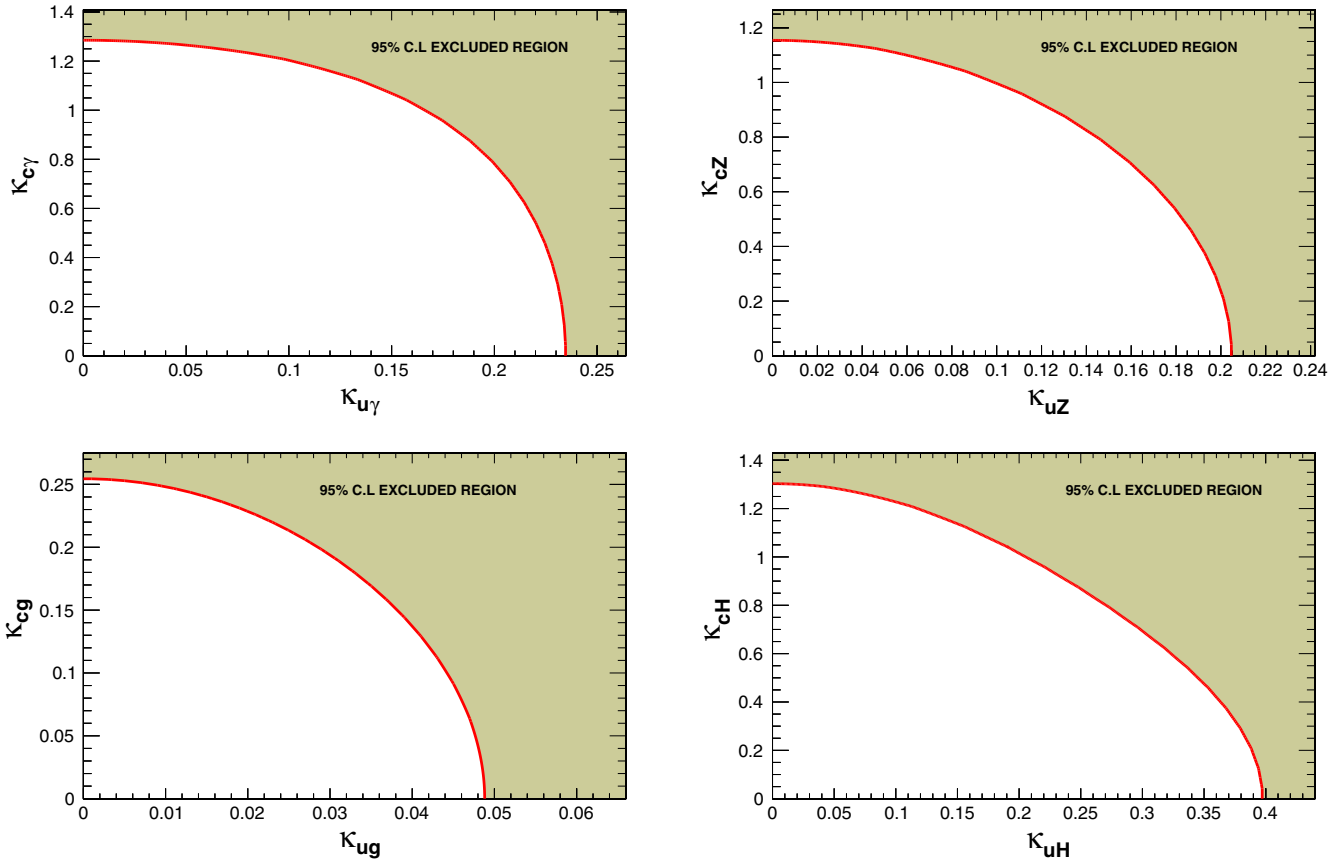

FIG. 3 (color online). Excluded region at 95% C.L. in the $\kappa_{uX} - \kappa_{cX}$ plane for $X = \gamma$, Z, gluon, and Higgs.

The same-sign analysis used to constrain the top-quark FCNC interactions has three sources of SM background:

(i) Fake leptons, i.e., the selected leptons do not originate from either the decay of a boson or the decay of a τ lepton.
(ii) Charge flips, i.e., the electron charge is mismeasured due to severe bremsstrahlung in the tracker material.
(iii) Rare SM processes, which mostly come from $t\bar{t}W$ and $t\bar{t}Z$.

The contributions of these three sources are reported separately in Ref. [27]. The simulation does not properly reproduce the contribution of the backgrounds with fake or charge-flipped leptons (instrumental background). Therefore, data-driven methods were used to estimate the instrumental background contribution from data in Ref. [27]. In addition to the considerable contribution of these backgrounds, they are also the main source of uncertainties. However, this makes it impossible to precisely predict the expected limit for higher center-of-mass energies or an arbitrary luminosity.

To estimate the reach of the search for FCNC anomalous production of same-sign top quarks at the 14 TeV LHC using the results of a search identical to the CMS search at 8 TeV [27], we need to estimate the contribution of the instrumental and rare SM backgrounds at the 14 TeV LHC. The method (which was developed in Sec. 3 of Ref. [41]) is used to estimate the contribution of instrumental backgrounds. The idea is as follows. Due to the final selection criteria (especially the two b-jets requirement), $t\bar{t}$ is the main source of instrumental background. So one can scale the rate of these backgrounds with the $t\bar{t}$ cross section approximately and predict their contributions at 14 TeV. To estimate the contribution of the rare SM backgrounds, we first produce the $t\bar{t}W$ and $t\bar{t}Z$ samples at 14 TeV using MADGRAPH5 [35]. We then use PYTHIA [39] and DELPHES [40] to simulate the showering, hadronization, and detector effects with the same condition explained in Sec. III B. Finally, the same cuts as mentioned before are imposed to find the number of events from $t\bar{t}W$ and $t\bar{t}Z$ in SR2.

The prediction of the expected backgrounds at 14 TeV is validated by calculating the ratio of the instrumental background to the rare SM backgrounds for SR6 and SR8 and comparing them with the ratios calculated in Ref. [41]. The ratios are fully compatible in both regions, and it is calculated to be 2.02 for SR2.

In order to estimate the uncertainties of instrumental backgrounds, no detector simulation is performed. The uncertainty obtained from 8 TeV is scaled according to the $t\bar{t}$ cross section to evaluate the uncertainty at 14 TeV, which leads to a large uncertainty. It would make our analysis

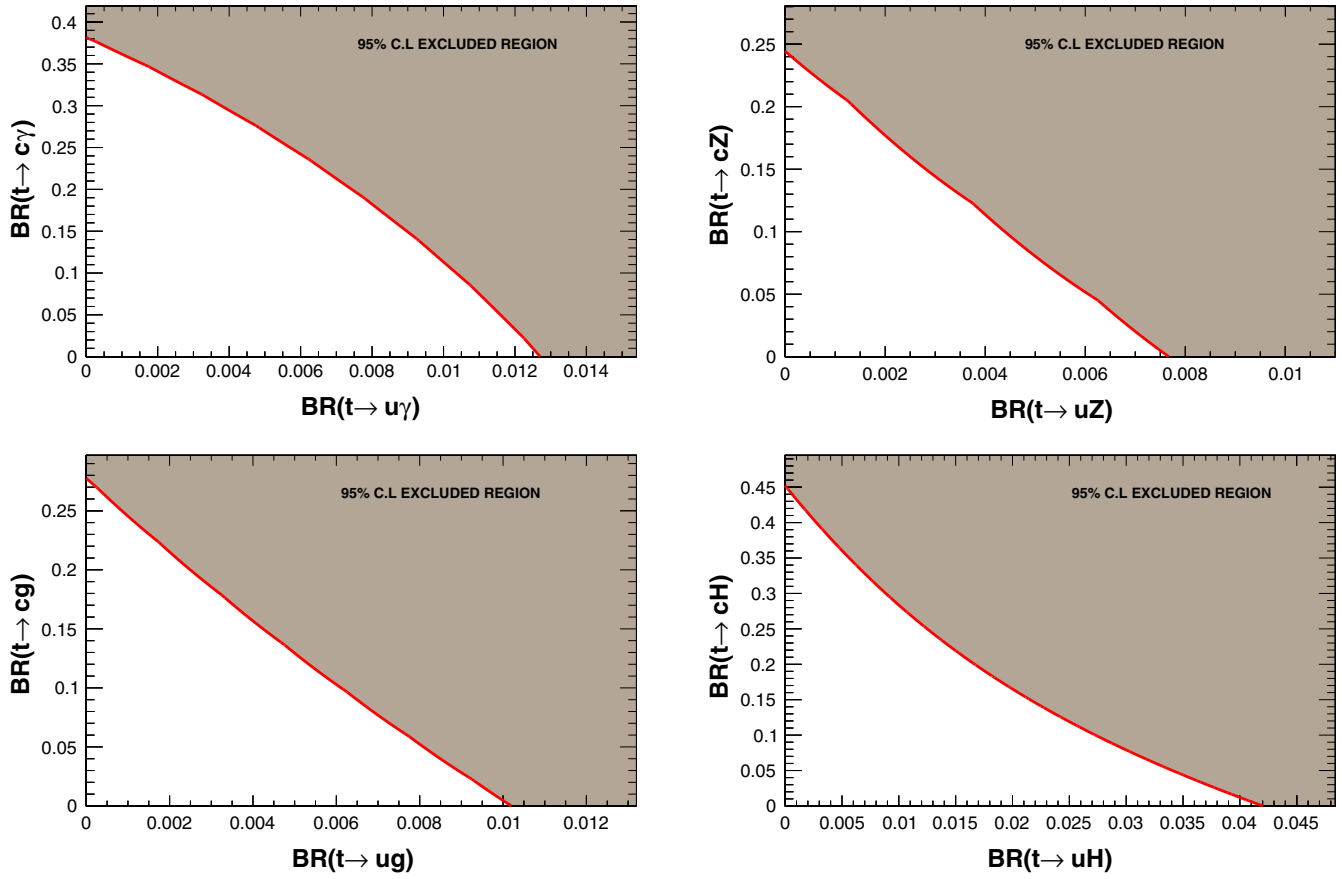

FIG. 4 (color online). Excluded region at 95% C.L. in the $\mathrm{BR}(t \to uX) - \mathrm{BR}(t \to cX)$ plane for $X = \gamma$, Z, gluon, and Higgs.

more useful if we could present the results considering different uncertainties from instrumental backgrounds. In order to illustrate the uncertainty effects, we define

$$\zeta = \frac{\text{Total background rate}}{\text{Irreducible background rate}} = 1 + \frac{\text{Instrumental background rate}}{\text{Irreducible background rate}}, \quad (5)$$

where both rates are calculated after all cuts. Combining the rare SM and instrumental backgrounds, the 95% predicted exclusion limits are presented in Fig. 6 for all signal channels. The ζ is varied between 1 to 10 to show how the reach of the analysis would change by changing the uncertainty on the instrumental backgrounds. Using the nominal value for $\zeta = 3.02$, it can be seen that the 95% excluded region boundaries have not improved significantly at the 14 TeV LHC compared to the 8 TeV LHC for the $tu\gamma$, tuZ, and tug signal channels, and the reach is even worse for tuH.

The CMS Collaboration has updated the same-sign analysis with 19.5 fb^{-1} of data [42]. The total uncertainties are increased in different signal regions by increasing the luminosity from 10.5 fb^{-1} to 19.5 fb^{-1}. Our studies show that using updated experimental results would not change the results obtained in this analysis. This behavior confirms that scaling the instrumental background rates and their related uncertainties to the $t\bar{t}$ cross section is a good approximation.

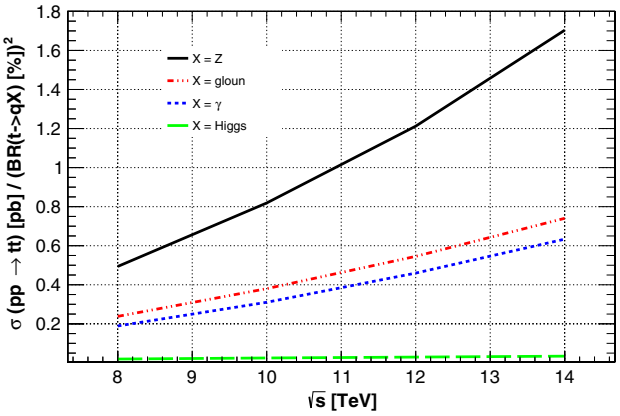

FIG. 5 (color online). Anomalous top pair-production cross section for the process $pp \to tt$ due to tuX anomalous vertices divided by the square of the FCNC branching ratios for the decays $\mathrm{BR}(t \to q\gamma)$, $\mathrm{BR}(t \to qZ)$, $\mathrm{BR}(t \to qg)$, and $\mathrm{BR}(t \to qH)$ versus the center-of-mass energy.

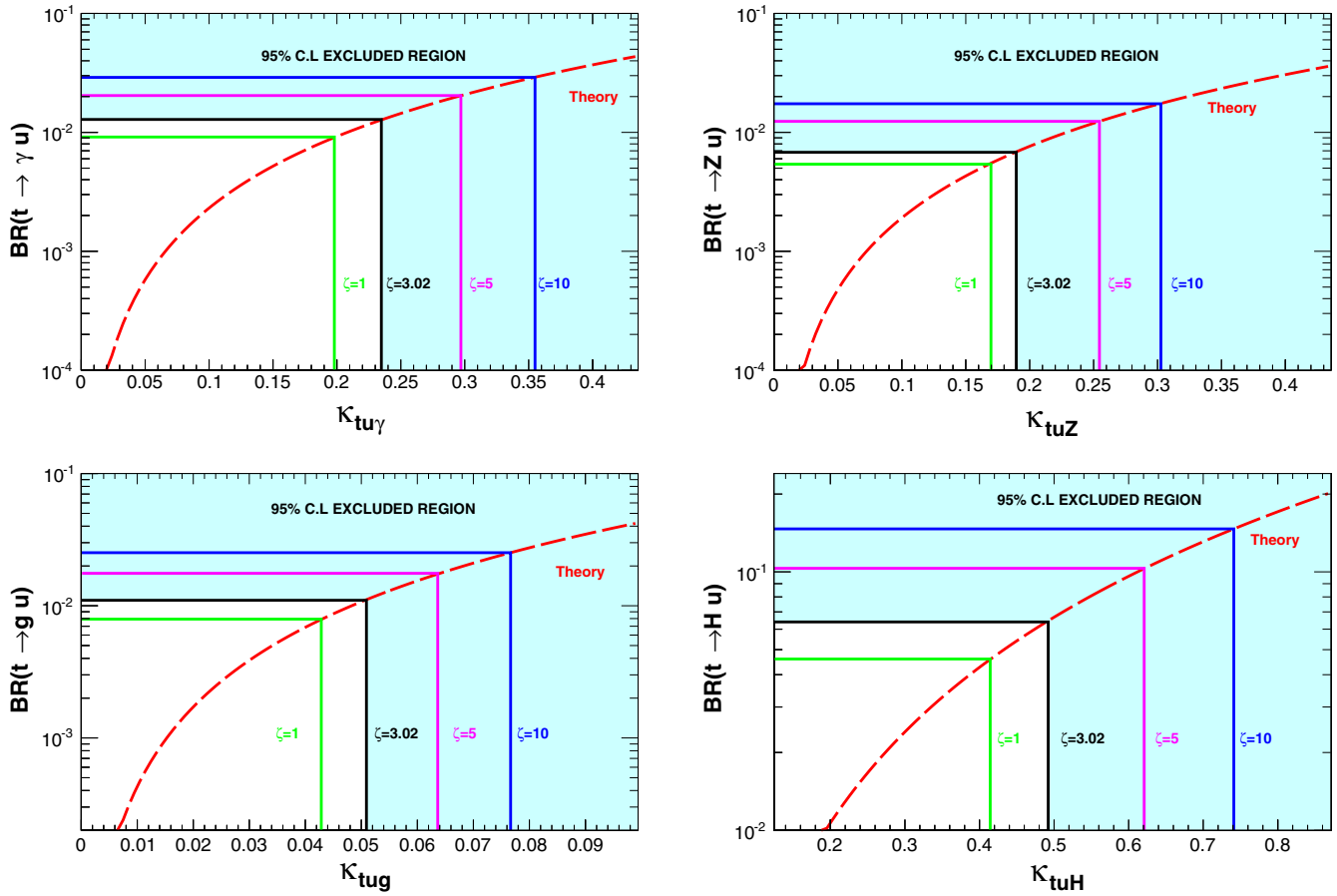

FIG. 6 (color online). Estimated 95% C.L. expected exclusion reach of flavor-violating top-Z, top-photon, top-gluon, or top-Higgs couplings and the related top-quark branching ratio through the same-sign top-channel signature at the 14 TeV LHC with 100 fb^{-1}. Concerning the important effect of the instrumental background on the predicted results, a range is assumed for ζ. $\zeta = 3.02$ is obtained by rescaling the experimental result in SR2 at 8 TeV. The theoretical prediction for the top-quark FCNC branching ratios versus the anomalous couplings are also shown.

VI. DISCUSSION AND CONCLUSIONS

In this work, we have analyzed the same-sign top-quark pair signature of the top-quark flavor-changing neutral interactions through photon, Z-boson, gluon, and Higgs boson exchanges in proton-proton collisions. The experimental results obtained by CMS at a center-of-mass energy of 8 TeV were used to constrain the top-quark anomalous couplings and branching ratios.

Whereas the limits obtained on the FCNC branching ratios of top-quark decays are found to be noncompetitive compared to recent results derived from anomalous single top-quark production or the anomalous decay of a top quark in $t\bar{t}$ events [11,15,18,20,21,43–45], these results provide an interesting cross-check of the evidences for the absence of the top-quark FCNC interactions in a different physics process.

The limits could be improved if the CMS Collaboration updates the same-sign dilepton search by subdividing the signal regions exclusively, so the results from different signal regions could be combined. An improvement of the lepton and b-tag efficiencies and the systematic uncertainties on the background predictions would improve the results.

Using the results of the CMS same-sign dilepton search at 8 TeV [27], we tried to predict the possible reach of the 14 TeV LHC. However, the presence of the instrumental backgrounds as an important source of uncertainties makes the prediction of the analysis reach vague. We find that with selections identical to the 8 TeV search no significant improvement is expected to be obtained for the top-quark FCNC process through the same-sign dilepton signature at the 14 TeV LHC.

ACKNOWLEDGMENTS

The author thanks Mojtaba Mohammadi Najafabadi for useful discussions and comments on the manuscript.

[1] W. Bernreuther, J. Phys. G **35**, 083001 (2008).
[2] S. Glashow, J. Iliopoulos, and L. Maiani, Phys. Rev. D **2**, 1285 (1970).
[3] J. Aguilar-Saavedra, Acta Phys. Pol. B **35**, 2695 (2004).
[4] J. Cao, C. Han, L. Wu, J. M. Yang, and M. Zhang, Eur. Phys. J. C **74**, 3058 (2014).
[5] A. Dedes, M. Paraskevas, J. Rosiek, K. Suxho, and K. Tamvakis, J. High Energy Phys. 11 (2014) 137.
[6] J. Cao, G. Eilam, M. Frank, K. Hikasa, G. Liu, I. Turan, and J. Yang, Phys. Rev. D **75**, 075021 (2007).
[7] G. Eilam, A. Gemintern, T. Han, J. Yang, and X. Zhang, Phys. Lett. B **510**, 227 (2001).
[8] D. Atwood, L. Reina, and A. Soni, Phys. Rev. D **55**, 3156 (1997).
[9] G.-r. Lu, F.-r. Yin, X.-l. Wang, and L.-d. Wan, Phys. Rev. D **68**, 015002 (2003).
[10] F. Abe *et al.* (CDF Collaboration), Phys. Rev. Lett. **80**, 2525 (1998).
[11] S. Chatrchyan *et al.* (CMS Collaboration), Report No. CMS-PAS-TOP-14-003.
[12] T. Aaltonen *et al.* (CDF Collaboration), Phys. Rev. Lett. **101**, 192002 (2008).
[13] V. M. Abazov *et al.* (D0 Collaboration), Phys. Lett. B **701**, 313 (2011).
[14] G. Aad *et al.* (ATLAS Collaboration), J. High Energy Phys. 09 (2012) 139.
[15] S. Chatrchyan *et al.* (CMS Collaboration), Phys. Rev. Lett. **112**, 171802 (2014).
[16] T. Aaltonen *et al.* (CDF Collaboration), Phys. Rev. Lett. **102**, 151801 (2009).
[17] V. M. Abazov *et al.* (D0 Collaboration), Phys. Lett. B **693**, 81 (2010).
[18] G. Aad *et al.* (ATLAS Collaboration), Report No. ATLAS-CONF-2013-063, ATLAS-COM-CONF-2013-064.
[19] S. Chatrchyan *et al.* (CMS Collaboration), Report No. CMS-PAS-TOP-14-007.
[20] G. Aad *et al.* (ATLAS Collaboration), J. High Energy Phys. 06 (2014) 008.
[21] S. Chatrchyan *et al.* (CMS Collaboration), Report No. CMS-PAS-HIG-13-034.
[22] Y. Gouz and S. Slabospitsky, Phys. Lett. B **457**, 177 (1999).
[23] D. Atwood, S. K. Gupta, and A. Soni, J. High Energy Phys. 10 (2014) 057.
[24] M. Khatiri Yanehsari, S. Jafari, and M. Mohammadi Najafabadi, Int. J. Theor. Phys. **52**, 4229 (2013).
[25] S. Chatrchyan *et al.* (CMS Collaboration), J. High Energy Phys. 08 (2011) 005.
[26] D. Atwood, S. K. Gupta, and A. Soni, J. High Energy Phys. 04 (2013) 035.
[27] S. Chatrchyan *et al.* (CMS Collaboration), J. High Energy Phys. 03 (2013) 037.
[28] R. Contino and G. Servant, J. High Energy Phys. 06 (2008) 026.
[29] J. Cao, L. Wang, L. Wu, and J. M. Yang, Phys. Rev. D **84**, 074001 (2011).
[30] E. L. Berger, Q.-H. Cao, C.-R. Chen, C. S. Li, and H. Zhang, Phys. Rev. Lett. **106**, 201801 (2011).
[31] H.-C. Cheng, K. T. Matchev, and M. Schmaltz, Phys. Rev. D **66**, 056006 (2002).
[32] M. Cacciari, G. P. Salam, and G. Soyez, J. High Energy Phys. 04 (2008) 063.
[33] S. Chatrchyan *et al.* (CMS Collaboration), JINST **8**, P04013 (2013).
[34] A. Alloul, N. D. Christensen, C. Degrande, C. Duhr, and B. Fuks, Comput. Phys. Commun. **185**, 2250 (2014).
[35] J. Alwall, M. Herquet, F. Maltoni, O. Mattelaer, and T. Stelzer, J. High Energy Phys. 06 (2011) 128.
[36] C. Degrande, C. Duhr, B. Fuks, D. Grellscheid, O. Mattelaer, and T. Reiter, Comput. Phys. Commun. **183**, 1201 (2012).
[37] J. Aguilar-Saavedra, Nucl. Phys. **B821**, 215 (2009).
[38] S. Khatibi and M. M. Najafabadi, Phys. Rev. D **89**, 054011 (2014).
[39] T. Sjostrand, S. Mrenna, and P. Z. Skands, J. High Energy Phys. 05 (2006) 026.
[40] J. de Favereau, C. Delaere, P. Demin, A. Giammanco, V. Lemaître, A. Mertens, and M. Selvaggi (DELPHES 3 Collaboration), J. High Energy Phys. 02 (2014) 057.
[41] J. Berger, M. Perelstein, M. Saelim, and P. Tanedo, J. High Energy Phys. 04 (2013) 077.
[42] S. Chatrchyan *et al.* (CMS Collaboration), J. High Energy Phys. 01 (2014) 163.
[43] S. Chatrchyan *et al.* (CMS Collaboration), Phys. Rev. D **90**, 032006 (2014).
[44] N. Craig, J. A. Evans, R. Gray, M. Park, S. Somalwar, S. Thomas, and M. Walker, Phys. Rev. D **86**, 075002 (2012).
[45] A. Greljo, J. F. Kamenik, and J. Kopp, J. High Energy Phys. 07 (2014) 046.